JOURNAL OF MATERIALS SCIENCE 26 (1991) 2417–2420

The hP1-type phases in alloys of cadmium, mercury, and indium with tin

G. C. CHE, M. ELLNER, K. SCHUBERT
Max-Planck-Institut für Metallforschung, Institut für Werkstoffwissenschaft, Seestraße 92, D-7000 Stuttgart, FRG

The hP1-type phases in alloys of Cd, Hg, and In with Sn are stable in the valence electron concentration interval 3.80–3.95. Following a rule of Raynor, the axial ratio c/a decreases with increasing valence electron concentration, N_b^{at}. Using lattice constant measurements the rule is confirmed, and by using density measurements the absence of constitutional vacancies is verified. The $c/a \rightarrow N_b^{at}$ relation of the hP1 phases is similar to $c/a \rightarrow N_b^{at}$ of $InSn_m$ ($0 < m < 0.1$) and In_3Sn. A bonding-type proposal, explaining the stability of these structures and the dependence of their axial ratio on valence electron concentration, is derived.

1. Introduction

The hP1 structure was first found in $HgSn_{12}$ [1, 2], extending up to $HgSn_6$ [3] so that the nominal composition $HgSn_9$ may be chosen, then in $InSn_4$ [4] and in $CdSn_{19}$.h [3, 5]. The varying composition of the hP1 phases shows that their structures are disordered. By fast cooling to 83 K, further phases were obtained: $TlSn_4$.m [6], In_3Bi_2.m, $InBi_2$.m [7], $Cu_{35}Sn_{65}$.m, $Ag_{04}Sn_{96}$.m, $Au_{08}Sn_{92}$.m, $Zn_{15}Sn_{85}$.m, $Cd_{30}Sn_{70}$.m, $Al_{50}Sn_{50}$.m, $Ga_{20}Sn_{80}$.m, and also $Mg_{15}Sn_{85}$.m, $Ca_{15}Sn_{85}$.m, $Pd_{08}Sn_{92}$.m, $Pb_{26}Sn_{74}$.m [8]; near 210 K the phases transform to the equilibrium state. A survey of homologic mixtures [9] shows that the Po and the Sn.r type also occur in these alloys. A topological diagram advanced by Giessen [10] provides intuitive structure fields. The fact that the axial ratio c/a of the stable phases decreases uniformly with increasing valence electron concentration [5] may be named Raynors rule. Most of the above metastable phases also obey Raynors rule, but for phases containing Mg, Ca, Pd, Pb, *ad hoc* valencies had to be chosen to fit them to the rule. Raynors rule is remarkable because it contradicts the strain rule [11], stating that with increasing valence electron concentration, a strain along a 4- or 6-axis frequently occurs, because in the basal plane a good commensurability of the valence electron correlation to the structure exists, while in the direction of the axis, additional correlation planes are inserted (see Section 4).

In order to understand Raynors rule energetically, it was desirable to confirm it by independent lattice constant measurements. Furthermore, it was necessary to confirm by density measurements that no constitutional vacancies are in the cell so that the valence electron concentration incidentally is the number of valence electrons in the cell. In connection with these experimental data, a model providing energetical arguments for Raynors rule will be explained in Section 4.

2. Experimental procedure

Alloys consisting of cadmium, mercury, indium and tin (all Preussag containing more than 99.999%) were melted in evacuated, then argon (Messer-Griesheim 5.0) filled and sealed silica ampoules. The alloys were generally homogenized at 100 °C for 7 days and slowly cooled. Because a significant weight loss of melted alloys was not observed, chemical analysis was not carried out. Bulk alloys were filed for powder diffraction. For splat cooling, a shock-wave tube [12] was used. Powder diffraction photographs were recorded using a Debye–Scherrer camera (diameter = 114.8 mm) and in a Guinier camera (Enraf-Nonius FR 552) using CuK_{α_1} radiation. For Guinier photographs, silicon was used as an internal calibration standard. For the high-temperature X-ray powder diffraction measurements, a Guinier–Simon camera (Enraf-Nonius FR 553) with CuK_{α_1} radiation was used.

The lattice parameters were refined by a least squares calculation using all observed reflections. The powder intensities were calculated using the program LAZY PULVERIX [13]. Mass densities of bulk alloys were measured by means of the loss-of-weight method with CCl_4 as liquid.

3. Results

High-temperature photographs of $Cd_{0.05}Sn_{0.95}$ at 175 °C showed the $HgSn_9$(hP1)-type structure. Experimental results, together with results taken from the literature, are collected in Table I. For the purpose of identification, the powder data are given in Table II.

Guinier room-temperature photographs for the tin-rich alloys near $HgSn_9$ suggest the existence of a single-phase hP1 structure for the mole fractions $x_{Sn} = 0.88$–0.92 where the small value is uncertain because Hg is liquid. The dependence of lattice constants on x_{Sn} was calculated from the Debye–Scherrer photographs and are given in Table I. X-ray data for

0022–2461/91 $03.00 + .12

TABLE I Some alloys containing a hP1 phase, their lattice data and valence electron concentration N_b^{at}

Alloy comp. (mole fract.)		Temp. of alloy (°C)	Latt. const. of hP1		Phases contained	c/a of hP1 phase	N_b^{at} of actual hP1 phase	Reference
			a (nm)	c (nm)				
Cd	Sn							
0.10	0.90	180	0.323 9(2)	0.301 2(2)	liq. + $CdSn_{19}$.h	0.939 9(8)	3.90	Present work
0.05	0.95	175	0.324 0(2)	0.300 9(2)	$CdSn_{19}$.h	0.928 4(8)	3.90	Present work
0.049	0.951	176	0.323 28	0.300 24	$CdSn_{19}$.h	0.928 7	3.902	[5]
Hg	Sn							
0.11	0.89	25	0.320 65(6)	0.298 60(7)	$HgSn_9$	0.931 2(2)	3.78	Present work
0.10	0.90	25	0.320 74(6)	0.298 65(9)	$HgSn_9$	0.931 1(3)	3.80	Present work
0.09	0.91	25	0.320 89(5)	0.298 75(7)	$HgSn_9$	0.931 0(2)	3.82	Present work
0.072	0.928	25	0.321 27	0.299 16	$HgSn_9$	0.931 2	3.856	[5]
0.07	0.93	25	0.321 09(5)	0.298 88(6)	$HgSn_9$ + βSn	0.930 8(2)	3.86	Present work
0.035	0.965	188	0.324 15	0.300 66	$HgSn_9$.h	0.927 5	3.93	[5]
In	Sn							
0.223	0.777	25.6	0.321 60	0.299 77	$InSn_4$	0.932 1		[1]
0.22	0.78	25	0.321 58(5)	0.299 72(9)	In_3Sn + $InSn_4$	0.932 0(3)		Present work
0.20	0.80	25	0.321 59(6)	0.299 72(8)	$InSn_4$	0.932 0(3)	3.80	Present work
0.193	0.807	25.6	0.321 74	0.299 80	$InSn_4$	0.931 8	3.807	[1]
0.186	0.814	25	0.321 77	0.299 88	$InSn_4$	0.932 0	3.81	[5]
0.18	0.82	25	0.321 72(4)	0.299 83(7)	$InSn_4$	0.932 0(2)	3.82	Present work
0.164	0.836	26.3	0.321 85	0.299 83	$InSn_4$	0.931 6	3.836	[1]
0.16	0.84	25	0.321 76(4)	0.299 92(7)	$InSn_4$	0.932 1(2)	3.84	Present work
0.14	0.86	25	0.321 89(4)	0.300 11(8)	$InSn_4$ + βSn	0.932 3(3)		Present work

TABLE II X-ray powder diffraction data for $CdSn_{19}$. Experiment: $Cd_{05}Sn_{95}$ at 175 °C in Guinier–Simon camera. Structure: $HgSn_9$, P6/mmm, 0.05Cd + 0.95 Sn in (a): 0.0.0; $a = 0.324\,0(2)$, $c = 0.300\,9(2)$ nm

hkl	$d_{cal.}$(nm)	$d_{obs.}$(nm)	$I_{obs.}$	$I_{cal.}$
0 0 1	0.300 90	0.300 35	m	40
1 0 0	0.280 59	0.280 31	vvs	100
1 0 1	0.205 21	0.205 00	vs	81
1 1 0	0.162 00	0.161 89	w	19
0 0 2	0.150 45	0.150 34	vvw	5
1 1 1	0.142 64	0.142 46	mw	24
2 0 0	0.140 30	0.140 37	vw	11
1 0 2	0.132 59	0.132 65	w	19
2 0 1	0.127 15	0.127 17	w	16

identification and also mass density for $HgSn_9$ at $x_{Sn} = 0.90$ are given in Table III. Measured lattice constants and density confirm the number of atoms in the unit cell $N_A^C = 0.994 \approx 1.0$.

For the In–Sn system, the $HgSn_9$(hP1)-type structure was found to be homogeneous at $x_{Sn} = 0.80$–0.84. The dependence of lattice data on mole fraction is shown in Table I. X-ray data for identification and density values for $In_{0.20}Sn_{0.80}$ are shown in Table IV. The experimental values confirm the expected number of atoms in the unit cell $N_A^C = 0.985 \approx 1.0$.

An error was found in the ASTM identification card 7-396 displaying the number of atoms in the hexagonal unit cell $N_A^C = 5$ (5H) instead of $N_A^C = 1$. As to be expected, splat cooling ZnSn, Pb_3Sb, Sn_3Bi, Tl_2Sn_3, In_7Sb_3, In_3Sb_7 from the melt to room temperature did not yield hP1 phases. The dependence of axial ratio c/a on the valence electron concentration for stable phases with hP1 structure (Raynors rule) is shown in Fig. 1.

TABLE III X-ray powder diffraction data for $HgSn_9$. Experiment: $Hg_{10}Sn_{90}$, room temperature, Debye camera. Structure: $HgSn_9$, P6/mmm, 0.1 Hg + 0.9 Sn (a) 0.0.0; $a = 0.320\,74(6)$, $c = 0.298\,65(9)$ nm. Mass density: $D_m = 7.89 \times \mathrm{Mg\,m^{-3}}$ number of atoms per cell = 0.994

hkl	$d_{cal.}$(nm)	$d_{obs.}$(nm)	$I_{obs.}$	$I_{cal.}$
0 0 1	0.298 65	0.299 16	m	40
1 0 0	0.277 77	0.278 25	vvs	100
1 0 1	0.203 39	0.203 39	vs	81
1 1 0	0.160 37	0.160 37	w	19
0 0 2	0.149 32	0.149 41	vvw	5
1 1 1	0.141 29	0.141 42	w	24
2 0 0	0.138 88	0.139 04	vw	12
1 0 2	0.131 52	0.131 68	w	19
2 0 1	0.125 93	0.126 02	w	17
1 1 2	0.109 28	0.109 16	vw	11
2 1 0	0.104 99	0.104 99	vw	10
2 0 2	0.101 70	0.101 71	vw	10
0 0 3	0.099 55	–	–	2
2 1 1	0.099 05	0.099 00	w	19
1 0 3	0.093 71	0.093 70	vw	9
3 0 0	0.092 59	0.092 53	vvw	5
3 0 1	0.088 44	0.088 45	vw	10
2 1 2	0.085 88	0.085 86	w	22
1 1 3	0.084 58	0.084 55	vw	12
2 0 3	0.080 91	0.080 90	w	16
2 2 0	0.080 19	0.080 19	vvw	9
3 0 2	0.078 69	0.078 70	w	24
2 2 1	0.077 44	0.077 44	m	48

4. Discussion

With respect to the stability of the $HgSn_9$ structure, it appears of interest to know the bonding type provided by the electron correlations model [14] for this phase. The mixture In–Sn appears especially appropriate for a bonding-type analysis because of the close relation between its components in the periodic system of elements. A bonding type may be described by lattice-like spatial correlations in the gas of the valence

TABLE IV X-ray powder diffraction data for $InSn_4$. Experiment: $In_{20}Sn_{80}$, room temperature, Debye camera. Structure: $HgSn_9$, P6/mmm, 0.2 In + 0.8 Sn (a) 0.0.0; $a = 0.321\,59(6)$, $c = 0.299\,72(8)$ nm. Mass density: $D_m = 7.18 \times$ Mg m^{-3} $N_{at}^{C} = 0.985$

hkl	$d_{cal.}$ (nm)	$d_{obs.}$ (nm)	$I_{obs.}$	$I_{cal.}$
0 0 1	0.299 72	0.300 55	m	41
1 0 0	0.278 51	0.278 94	vvs	100
1 0 1	0.204 02	0.204 21	vs	81
1 1 0	0.160 80	0.160 96	w	19
0 0 2	0.149 86	0.149 90	vvw	5
1 1 1	0.141 69	0.141 73	w	24
2 0 0	0.139 25	0.139 41	vw	11
1 0 2	0.131 97	0.131 97	w	19
2 0 1	0.126 29	0.126 36	w	16
1 1 2	0.109 63	0.109 61	vw	11
2 1 0	0.105 27	0.105 33	vw	10
2 0 2	0.102 01	0.101 95	vw	9
0 0 3	0.099 91	–	vvw	2
2 1 1	0.099 32	0.099 27	w	18
1 0 3	0.094 04	0.093 98	vw	9
3 0 0	0.092 84	0.092 80	vvw	5
3 0 1	0.088 68	0.088 69	vw	10
2 1 2	0.086 14	0.086 13	w	21
1 1 3	0.084 86	0.084 87	vw	11
2 0 3	0.081 18	0.081 20	vw	15
2 2 0	0.080 40	0.080 41	vw	8
3 0 2	0.078 92	0.078 93	w	22
2 2 1	0.077 65	0.077 65	mw	37

electrons (correlation-cell b), in the gas of the d electrons (cell e), and in the gas of the core electrons (cell g). Between the b, e, and g correlations, energetically favourable commensurabilities must exist. These commensurabilities are expressed by a bonding-type equation [14]. Because energy is involved in correlations and commensurabilities, a bonding type provides a stability argument.

Indium has a U1-type structure, where U is the tetragonal body centred lattice, 1 is the number of atoms in the primitive part of U, and for type designation see [14]. The In(U1) structure is explained in ([15] Vol. 1, p. 24, Vol. 29, p. 120). The bonding-type equation is $a(6, 20, 36) = 0.325$; 0.495 nm $= b_F(1; 3/2) = e_B(2; 3) = g_C(4; 6)$. Here a is the cell matrix of In, (6, 20, 36) are the numbers of valence-, d-, and core-electrons per a cell, 0.325; 0.495 nm is the abbreviated numerical value of a, b_F is the cell of the valence electron correlation, being of the F1-type (f c c), (1;3/2)

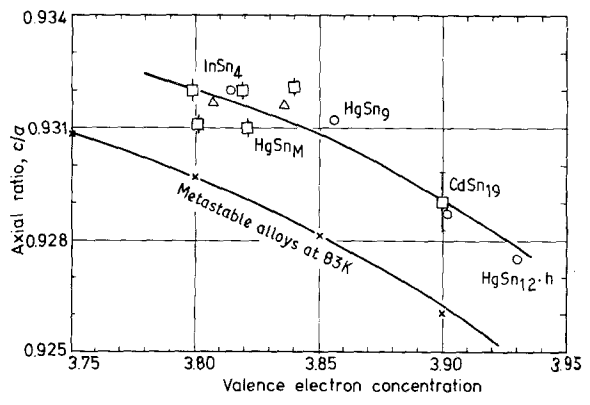

Figure 1 Axial ratio versus valence electron concentration for stable hP1 phases. (△) [1], (○) [5], (—) [8], (□) present work.

is the abbreviated commensurability $b^{-1}a$, e_B and g_C are the cells of the d- and core-electron correlations with types B1 (b c c) and C1 (primitive cubic) respectively, multiplied by the commensurabilities $e^{-1}a$ and $g^{-1}a$, respectively. For further comments on bonding types, see [14]. By calculation of the number of sites, it is seen that the b correlation is fully occupied but the e correlation has not sites enough for the b and e electrons together. Perhaps the bonding type is slightly compressed in the a_3 direction. The assumption that the b correlation is contained in the e correlation, is named the collective property of b and e, and it appears to be frequently fulfilled. The above proposal for the bonding type of In explains the special axial ratio of In. It also explains the change in axial ratio upon change of valence electron concentration (see [11], p. 173) by the above-mentioned strain mechanism. When with increasing Sn content the strain of the a cell becomes larger, the energy of the $InSn_m$ marginal phase is increased so that a change of the bonding type and therefore a change of the structure will take place in the next phase.

In_3Sn($SrPb_3$ type, T3.1, [15] Vol. 10, p. 59) is in equilibrium with In and has a tetragonally compressed Cu_3Au-type structure. The bonding type may be assumed as $a(13, 40, 72) = 0.486$; 0.440 nm $= b_{\breve{F}}(1.5; 15) = e_{\breve{B}}(3; 3) = g_{\breve{C}}(6; 6)$. Because the a cell is tetragonally compressed, b, e, g must also be compressed, and this is described by $\breve{F}$, $\breve{B}$, $\breve{C}$. Moreover the axial ratio $|a_3|/|a_1|$ decreases (see [15] Vol. 10, p. 59) with increasing number of b electrons per atom (b concentration N_b^{at}). The cause for this deformation of the bonding type must be sought in a spin compensation deforming $b_{\breve{F}}$ to a CuAu-type cell consisting of spin-up layers $(0\,0\,1)_{CuAu}$ alternating with spin-down layers. Because N_b^{at} increases from 3.25 towards 4 (not attaining this value) the spin compensation is improved and causes a continuous decrease of $|a_3|/|a_1|$. It is satisfactory that TlSn.h(CuAu, [15], Vol. 41, p. 13), [16], fits into the $|a_3|/|a_1| \rightarrow N_b^{at}$ relation of In_3Sn [16]. On the other hand, $In_3Pb(SrPb_3$, [15] Vol. 18, p. 172) has an $|a_3|/|a_1| \rightarrow N_b^{at}$ relation differing from that of In_3Sn [16]. It must be assumed here that the bonding type is slightly different: $a(13, 40, 76) = 0.490$; 0.455 nm $= b_F(2.5^{1/2}; 3/2) = e_B(10^{1/2}; 3) = g_C(40^{1/2}; 6)$. Here also, the correlations are compressed in the direction of the tetragonal axis because of spin compensation. The increase of the b site number has perhaps to do with the atomic radius difference of the components. $HgPb_2(SnPb_3$, [15] Vol. 18, p. 55) fits to In_3Pb [16], with $a(13.3, 40, 88) = 0.498$; 0.451 nm, not to In_3Sn.

$InSn_4$($HgSn_9$, H1, [15] Vol. 10, p. 59) has an $(0\,1\,0)$ plane similar to $(0\,0\,1)_{In_3Sn}$, but the stacking of the $(0\,1\,0)_{InSn_4}$ plane has the support number 2 (i.e. two atoms of a first layer support one atom of the next layer), while in In_3Sn it has the support number 4. Clearly, this is a consequence of the rule of the dependence of atomic volume on valence electron concentration in alloys between A^{10+n} components ([11], p. 169) following from the rule of full occupation of the b correlation [14] and the low compressibility of the correlations in these alloys. Because $|a_1| \approx |a_3|$, the

bonding type may be written for the quasi tetragonal aspect a' of the cell. $a(3.8,10,18)$ = H0.322; 0.300 nm, $a' = b_F(1;0.9) = e_B(2;1.8) = g_C(4;3.6)$, where H in the numerical value of a indicates the hexanormal basic coordinates, and $(-a_1 + a_2)/2$ is taken as a'_3 of the quasi tetragonal cell while $a'_1 = a_1 + a_2$ and $a'_2 = a_3$. In this bonding type, $|a_3|/|a_1| < 1$ must be caused by spin compensation in b forming a CuAu-type. Just as in In_3Sn the ratio $|a_3|/|a_1|$ decreases with increasing N_b^{at}, also in $InSn_4$ $|a_3|/|a_1|$ decreases with increasing N_b^{at} (see [15] Vol. 10, p. 60). The reason why a'_2 is just the c-axis of CuAu, lies in the crystal chemistry rule that high coordination favours larger distances and *vice versa*. In the next phase a support number 1 of quadratic layers might be expected; however, the influence of the electron correlations generates a more complicated homeotype of the Hg_9Sn type.

Sn.r(U2, [15] Vol. 1, p. 56), the room-temperature phase of Sn, has a tetragonal body-centred cell (U) with two atoms in the primitive part of the cell. It is homeotypic to Po(C1) by an inhomogeneous deformation [10]. This kind of deformation suggests a certain rotation of the bonding type against the a cell. $a(16, 40, 72) = 0.583$; 0.318 nm $= b_{F'}(3.25^{1/2}; 1) = e_B(13^{1/2}; 2) = g_C(52^{1/2}; 4)$. A Hund-insertion [14] in b indicated by F′ may be the cause of the weak paramagnetism of Sn.r. Curiously, Sn.r and also the following Sn.l do not exhibit a clear indication of spin compensation in b, perhaps the low coordination number of the atoms spoils the CuAu-type of spin compensation. At lower temperature, b electrons are no longer excited to Hund insertion, so that the b site number per atom must increase.

Sn.l(Si,F2, [15] Vol. 1, p. 12), the low-temperature phase of Sn, has an Si-type of structure being face-centred cubic with two atoms in the primitive part of the cell. $a(32,80,144) = 0.649$ nm $= b_F(2) = e_B(4) = g_C(8)$.

All phases of the mixture In–Sn have an FB2C4 (or briefly FB2) bonding type, i.e. b is of the F1-type, e is of the B1-type and its edge must be doubled to be equal to b, and g is of the C1-type and its edge must be multiplied by 4. The phases of the mixture are caused by different commensurabilities of the bonding type to the crystal cell a. However, this appears to be a consequence of the close homologic relation of the components In and Sn. To see this, a mixture with less closely homologic components may be finally and briefly considered.

In_9Bi.h(In_3Sn, [17]), $a(12.8, 40, 74) = 0.491$; 0.450 nm $= b_{\tilde{F}}(1.5; 1.5) = e_{\tilde{B}}(3; 3) = g_{\tilde{C}}(6; 6)$.

In_2Bi(Ni_2In, [15] Vol. 22, p. 50) is a deformed ordering homeotype of $HgSn_9$ but with $c/a > 1$ so that the bonding type presumably will be different. $a(22, 60, 116)$ = H0.550; 0.658 nm $= b_{BH}(1.5; 9/3) = e_{CH}(3; 9/3) = g_{FH}(6; 9/3)$. BH is the hexagonal aspect of B1 and so on. There are only 20.25 b sites per cell in the proposal, therefore a may contain Bi/In replacing. If b and e are collective (i.e. the e lattice contains the b lattice) then there is a small overoccupation of the e correlation. Also this suggests atomic replacement. It appears that In_2Bi and also In_5Bi_3 and In_3Bi_2.m do not have a FB2 bonding type. This confirms the conjecture that the invariance of FB2 in In–Sn is somewhat exceptional.

In_5Bi_3(Cr_5B_3, U10.6, [15] Vol. 34, p. 31, drawing [11] p. 252]) $a(120, 320, 624) = 0.854$; 1.268 nm $= b_U(10^{1/2};6) = e_{FU}(40^{1/2};13/2) = g_B(80^{1/2};13)$. It is seen that b and e are not collective while e and g are so.

In_3Bi_2.m(W,[7]), $a(7.6,20,39) = 0.382$ nm $= b_B(1.5) = e_C(3) = g_F(3)$. The slight overoccupation of b suggests structural vacancies.

InBi(PbO.T2.2, [15] Vol. 11, p. 46) is homeotypic to CuAu by an inhomogeneous deformation, $a(16, 40, 80) = 0.502$;0.478 nm $= b_F(2.5^{1/2}; 1.5) = e_B(10^{1/2}; 3) = g_C(40^{1/2}; 6)$. The phase shows weak Hund-insertion.

In_2Bi_3.m($HgSn_9$H1 [7]), $a(4.2, 10, 20)$ = H0.332; 0.312 nm $= b_F(1; 0.9) = e_B(2; 1.8) = g_C(4; 3.6)$. The bonding type is written for the quasi tetragonal cell.

$InBi_3$.m(def.$HgSn_9$, [7]).

$InBi_4$.m(Sn.r, [7]), $a(18.4,40,85) = 0.615$;0.330 nm $= b_F(3.25^{1/2};1.1) = e_B(13^{1/2};2.2) = g_C(52^{1/2}; 4.4)$. This phase shows strong Hund-insertion, and also spin compensation.

The above bonding type proposals suggest that the phases of $A^{10+n}A_M^{10+n'}$ mixtures may be interpreted by the electron correlations model. To verify the necessity of a bonding type proposal the last version of the electron distances in the chemical elements [18] should be consulted, and a plot of the electron distances in the intermediate phases over the mole fraction should be derived from the proposals, see for instance [19].

References

1. C. V. SIMSON, *Z. Phys. Chem.* **109** (1924) 183, SR1.570.
2. S. STENBECK, *Z. Anorg. Chem.* **214** (1933) 16, SR3.645.
3. K. SCHUBERT, U. RÖSLER, W. MAHLER, E. DÖRRE and W. SCHÜTTE, *Z. Metallkde* **45** (1954) 643.
4. C. G. FINK, E. R. JETTE, S. KATZ and F. J. SCHNETTLER, *Trans. Electrochem. Soc.* **88** (1945) 229, SR10.59
5. G. V. RAYNOR and J. A. LEE, *Acta Metall.* **2** (1954) 616, SR18.179.
6. B. C. GIESSEN, J. M. VITEK and N. J. GRANT, *Metall. Trans.* **3** (1972) 2449, SR38.171.
7. B. C. GIESSEN, M. MORRIS and N. J. GRANT, *Trans. Metall. Soc. AIME* **239** (1967) 883.
8. R. H. KANE, B. C. GIESSEN and N. J. GRANT, *Acta Metall.* **14** (1966) 605.
9. W. F. DEGTJAREVA and JU. A. SKAKOW, *Kristallogr.* **21** (1976) 405.
10. B. C. GIESSEN, *Adv. X-Ray Anal.* **12** (1969) 23.
11. K. SCHUBERT, "Kristallstrukturen, zweikomp. Phasen", (Springer Verlag, Berlin 1964).
12. G. BUCHER, M. ELLNER, F. SOMMER and B. PREDEL, *Mh Chemie* **117** (1986) 1367.
13. K. YVON, W. JEITSCHKO and E. PARTHÉ, *J. Appl. Crystallogr.* **20** (1977) 73.
14. K. SCHUBERT, *Commun. Math. Chem.* **19** (1986) 287.
15. *Structure Reports.* **1** (1931), **10** (1953), **18** (1961), and **29** (1972).
16. M. ELLNER and B. PREDEL, *Z. Metallkde* **66** (1975) 503.
17. P. D. CURRIE, T. R. FINLAYSON and T. F. SMITH, *J. Less-Common Metals* **62** (1978) 13.
18. K. SCHUBERT, *Z. Metallkde* **80** (1989) 276.
19. *Idem., Z. Kristallogr.* **179** (1987) 187.

Received 2 October 1989
and accepted 9 April 1990